Materials Science-Poland, *Vol. 27*, *No. 1*, *2009*

Synthesis and characterisation of SnO_2 films obtained by a wet chemical process

S. MAJUMDER*

Department of Physics, Asansol Engineering College, Asansol 713304, India

SnO_2 thin films, being n-type semiconductors, have wide application in the field of sensor technology. They are obtained by a wet chemical process, using $SnCl_2 \cdot 2H_2O$ as a tin containing precursor. The films thus obtained were subjected to optical, X-ray diffraction (XRD), microstructural, FTIR and Raman studies.

Key words: *SnO_2; Raman spectra; FTIR*

1. Introduction

Metal oxide gas sensors have been the subject of many investigations during the past [1–7]. These materials change their conductivity due to adsorption and desorption of oxygen on the surface of metal oxide (MOX) and surface reactions between the absorbed oxygen and the detecting gases. Oxygen from air is chemisorbed as O^-, O_2^-, or O^{2-}. This adsorbed oxygen gets trapped at the grain boundary trap states, thereby increasing the grain boundary potential barrier. This culminates in an increase in resistivity of the material. For reducing gases, the trap states get depleted of charge carriers and thereby reduce the resistance through lowering of the potential barrier at the grain boundaries.

Among various metal oxides studied for gas sensor applications, SnO_2 has emerged as one of potentially the most useful materials. Numerous reports described how various properties of the material have relevance to various aspects of gas sensor applications. Tin oxide has the unique property of being both transparent and conducting material. Different techniques [1, 8, 9] were adopted to deposit SnO_2 coatings for sensor applications. The wet chemical method became the most favoured one due to scalability and cost-effectiveness.

*E-mail: smajumderaec@gmail.com

In this study, all wet chemical routes were adopted to deposit SnO_2 films onto soda lime glass substrates. Optical, FTIR and Raman studies were also carried out on these films.

2. Experimental details

Tin oxide films were deposited from a sol by the spin coating method. Soda lime glass slides were used as the substrates. The substrates were cleaned thoroughly with liquid detergents and distilled water followed by boiling in distilled water. The substrates were then subject to ultrasonic treatment in 2-propanol for 15 min, and finally degreased with 2-propanol vapour before drying.

Sol preparation and the colour of the sol are important for getting a reproducible final product. Analytical reagent grade $SnCl_2{\cdot}2H_2O$ was used as a starting material. 0.837 g of $SnCl_2{\cdot}2H_2O$ was refluxed and stirred with 10 ml of dehydrated ethanol at around 353 K for 3 h. The resultant sol was then allowed to cool down to room temperature. Stirring was continued till the cooling down process was completed. SnO_2 films were deposited onto cleaned glass substrates by the spin coating technique, and the films were immediately annealed at 773 K for 20 min in air. The films were taken out after being cooled down to room temperature. This process produced transparent and adherent SnO_2 films.

Scanning electron microscopy (SEM) and X-ray diffraction (XRD) using CuK_α line were used to obtain the microstructural data. The crystallinity of each film was calculated from XRD spectra by Scherrer's formula:

$$D_m = \frac{0.9\lambda}{\beta \cos\theta} \tag{1}$$

where D_m is the crystallite size, β the full-width at half maximum (FWHM) of a distinctive peak (rad), θ the Bragg angle and $\lambda = 0.154$ nm.

Optical studies were performed by measuring the transmittance and the absorbance in the wavelength region 200–900 nm at room temperature using a spectrophotometer Hitachi-U3410. The spectra were recorded with the resolution of $\lambda \approx 0.07$ nm, along with a photometric accuracy of $\pm 0.3\%$ for transmittance measurements. Raman spectra were recorded using a Renishaw inVia micro-Raman spectrometer, equipped with a 514 nm Argon laser. FTIR spectra were recorded in the 4000–400 cm^{-1} range, using a Nicolet^{TM}-380 FTIR.

3. Results and discussion

Figure 1 shows the scanning electron micrograph (SEM) of a representative SnO_2 film. The film appeared to be compact and rougher surface in nature. The average

grain sizes were measured to be between 200 nm and 250 nm for the films. It was noticed that there was a tendency of grain growth with increase in annealing temperature, which was a general physical phenomenon. The XRD spectra (Fig. 2) are characterized by the presence of stronger but broader characteristic peaks for SnO_2 located at 2θ =26.61°, 33.89°, 51.79° and 61.87° arising out of reflections from (110), (101), (211) and (310) planes, respectively. Crystal size was computed from Eq. (1) and from XRD data; it was found that the size was ca. 40 nm for deposited SnO_2 thin film.

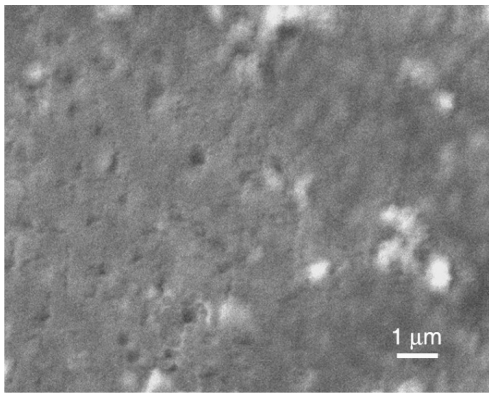

Fig. 1. SEM picture of as-deposited SnO_2 film

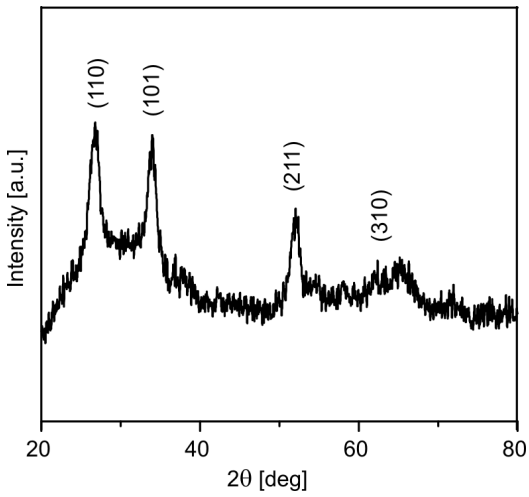

Fig. 2. XRD spectrum of the film
whose SEM picture shown in Fig. 1

The films were transparent in the visible region. The variation of the optical absorption coefficient α with photon energy $h\nu$ was obtained using the transmittance data for various films. The absorption coefficients α of the SnO_2 films were deter-

mined by measuring transmittance T_r and reflectance R in these films [10, 11]. The absorption coefficient α may be written as a function of the incident photon energy $h\nu$

$$\alpha = \frac{A}{h\nu}\left(h\nu - E_g\right)^m \tag{2}$$

where A is a constant which is different for different transitions indicated by different values of m, and E_g is the corresponding band gap. Equation (2) may be rewritten as:

$$\frac{d\left(\ln \alpha h\nu\right)}{d\left(h\nu\right)} = \frac{m}{h\nu - E_g} \tag{3}$$

A plot of $d(\ln(\alpha h\nu))/d(h\nu)$ vs. $h\nu$ will show a divergence at $h\nu = E_g$, from which a rough estimate of E_g may be obtained. Thus, by using Eq. (2), the value of m can easily be evaluated from the slope of the plot of $\ln(\alpha h\nu)$ vs. $\ln(h\nu - E_g)$. The inset of Fig. 3 shows the plot of $\ln(\alpha h\nu)$ vs. $\ln(h\nu - E_g)$ for a representative SnO_2 film. The value of m obtained from the slope is 0.46, which indicates that an allowed direct transition is present in deposited SnO_2 film. The band gap was determined by extrapolating the linear portion of the plot of $(\alpha h\nu)^2$ vs. hν (Fig. 3) which indicated $E_g \approx 3.66$ eV for the film.

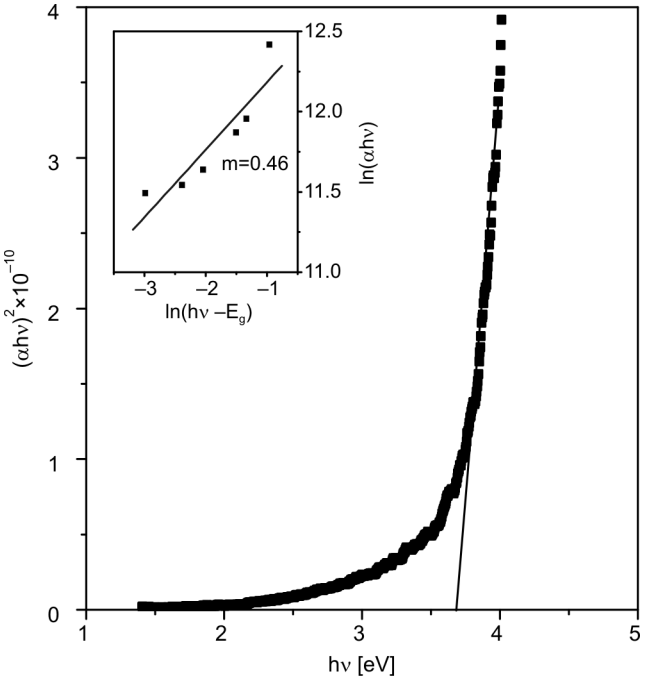

Fig. 3. Plots of $(\alpha h\nu)^2$ vs. hν for representative as-deposited SnO_2 film

FTIR and Raman studies were performed at room temperature on the SnO_2 film. The above studies reflected the bonding environment in these films. Figure 4 shows the FTIR spectra of the film. It may be observed that the SnO_2 film showed characteristic FTIR absorption peaks at ca. 511 cm^{-1} and 800 cm^{-1} which are due to Sn–O vibrational and O–Sn–O stretching modes, respectively. There are absorption peaks due to –CH, CO_2 and –OH modes. This observation is consistent with that reported by Chen and Gao [12].

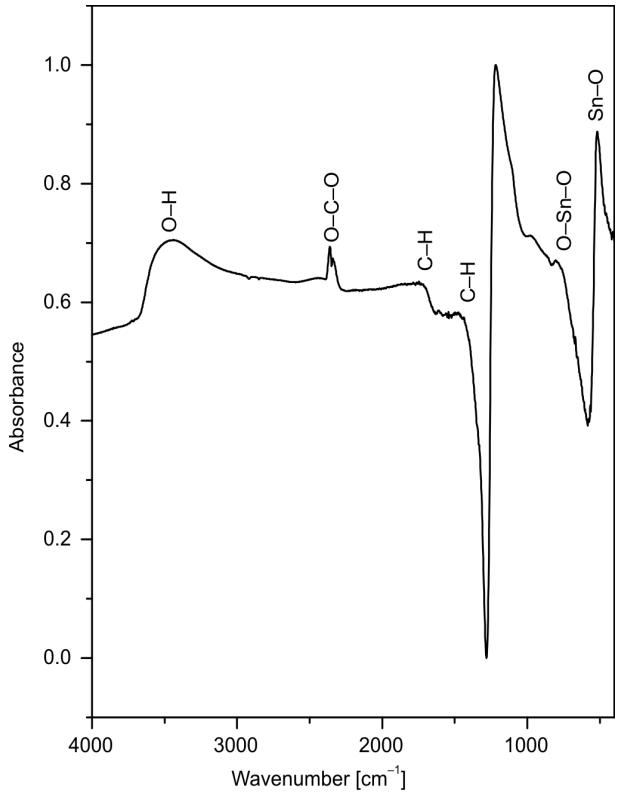

Fig. 4. FTIR for as-deposited SnO_2 film

Figure 5 shows typical Raman spectra for as-deposited SnO_2 film. The spectra for as-deposited SnO_2 is dominated by the presence of a broad and strong peak at ca. 560 cm^{-1} along with a peak of a smaller intensity at ca. 782 cm^{-1}. The peak at ca. 560 cm^{-1} has a shoulder and this peak, when deconvolved (inset of Fig. 5a), shows the existence of two peaks at ca. 567 cm^{-1} and 452 cm^{-1}. These two peaks could correspond to S1 and S2 bands of SnO_2, while the peak at ca. 782 cm^{-1} is due to B_{2g} mode of SnO_2. Similar Raman spectra of SnO_2 films have been reported in Refs. [13–15].

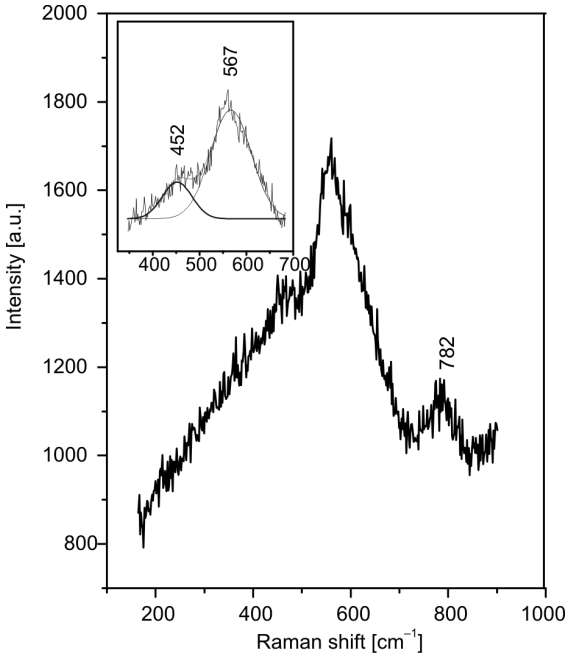

Fig. 5. Raman spectra for as-deposited SnO_2 film

4. Conclusion

SnO_2 films can be successfully obtained by the sol-gel technique. X-ray diffraction confirmed the presence of crystalline SnO_2 in these films. Tin (IV) oxide is non-stochiometric and is deficient in oxygen atoms. Charge neutrality is maintained by the presence of Sn^{2+} ions instead of Sn^{4+} ions. The Sn^{2+} ions act as electron donors during the process. At an elevated temperature, adsorption of atmospheric oxygen takes place by forming O_2^- , O^- or O^{2-} anions, thus decreasing the concentration of electrons near the surface and resulting in a depletion layer of higher resistance. Under exposure to reducing gases, the co-adsorption and interaction between gas and absorbed oxygen result in oxydation at the surface and a decrease in chemisorbed oxygen concentration, inducing an increase in conductance. Thus, SnO_2 may be used as a cheap gas sensing device for gases like methane, LPG, CO, NO_2. FTIR analysis indicated that the peaks for Sn–O at ca. 511 cm^{-1} became prominent and the peak due to stretching modes for O–Sn–O at ca. 800 cm^{-1} is prominent. This may possibly be due to the presence of very few oxygen vacant sites.

References

[1] SALEHI A., Thin Solid Films, 416 (2002), 260.
[2] KOHL D., J. Phys. D. Appl. Phys., 34 (2001), R125.

[3] MO Y., OKAWA Y., NAKAI T., TAJIMA M., NATUKAWA K., Thin Solid Films, 416 (2002), 248.
[4] GARDNER J.W., Sensors Actuators B, 4 (1991), 109.
[5] IMAWAN C., SOLZBACHER F., STEFFES H., OBERMEIER E., Sensors Actuators B, 68 (2000), 184.
[6] SCHWEBEL T., FLEISCHER M., MEIXNER H., Sensors Actuators B, 65 (2002), 176.
[7] HAHN S.H., BARSAN N., WEIMAR U., Sensors Actuators B, 78 (2001), 64.
[8] COBIANU C., SARANIU C., CICILIANO P., CAPONOE S., UTRIANIEN M., NINISTO L., Sensors Actuators B, 77 (2001), 496.
[9] GORDILLO G., MORENO L.C., DELA CRUZ W., TEHERAN P., Thin Solid Films, 252 (1994), 61.
[10] BHATTCHARYYA D., CHAUDHURI S., PAL A.K., Vacuum 4 (1992), 313.
[11] MOSS T.S., *Optical Properties of Semiconductors*, Butterworths, London, 1959, p. 34.
[12] CHEN D., GAO L., J. Colloid Interface Sci., 279 (2004), 137.
[13] PEERCY P.S., MOROSIN B., Phys. Rev. B, 7 (1973), 2279.
[14] DIEGUEZ A., ROMANO-RODRIGUEZ A., VILA A., MORANTE J.R., J. Appl. Phys., 90 (2001), 1550.
[15] YU K.N., XIONG Y., LIU Y., XIONG C., Phys. Rev. B, 55 (1997), 2666.

Received 23 December 2007
Revised 2 June 2008